**Supplementary Information for**

# A Peptide Uncoupling BDNF Receptor TrkB from Phospholipase Cγ1 Prevents Epilepsy Induced by Status Epilepticus

Bin Gu, Yang Zhong Huang, Xiao-Ping He, Rasesh B. Joshi, Wonjo Jang & James O. McNamara

## INDEX

**Figure S1**

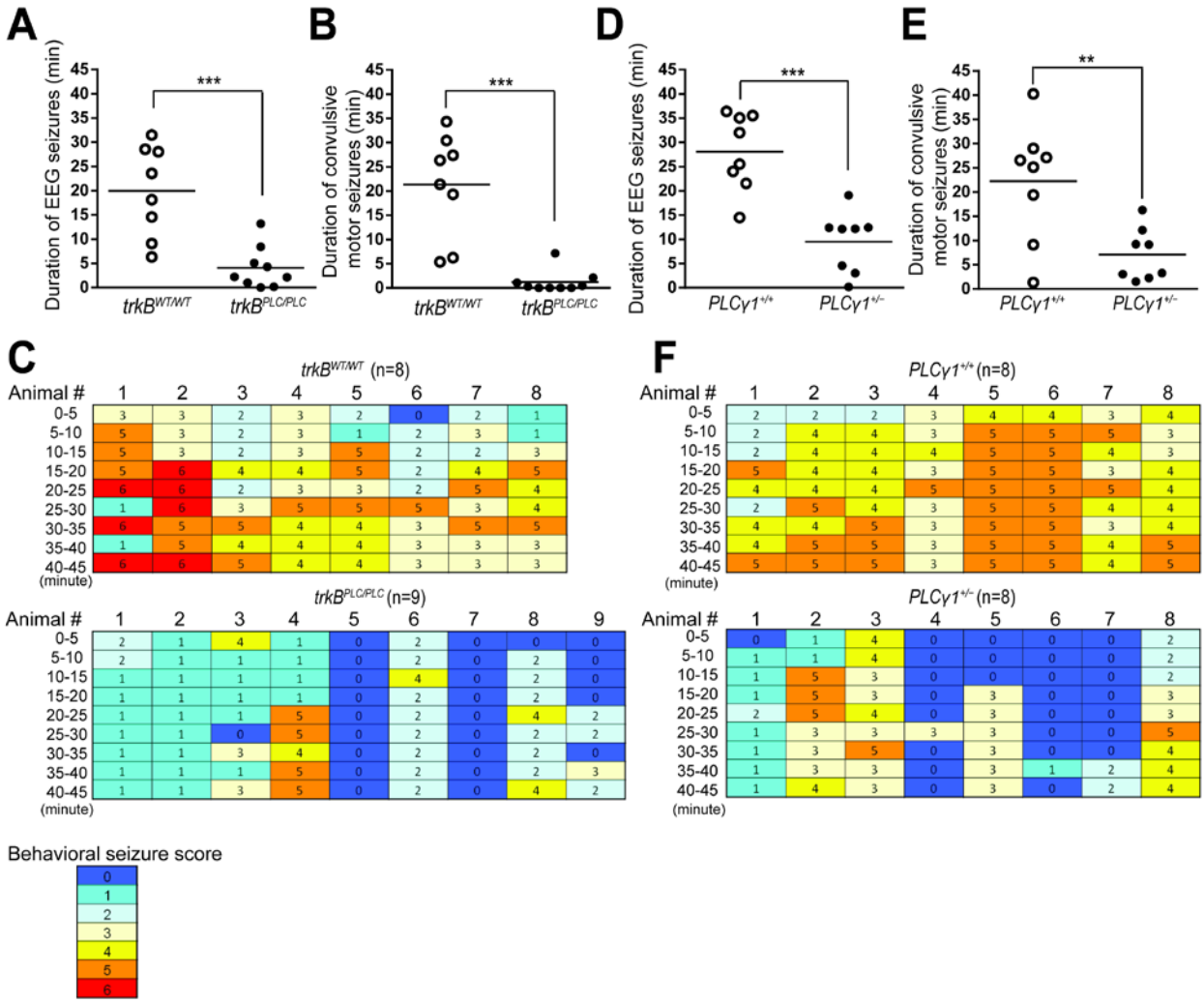


**Figure S1, Related to Figure 2. Disrupting TrkB-mediated PLCγ1 signaling inhibits chemoconvulsant-induced SE.**

(A-C) Genetically disrupting TrkB-mediated PLCγ1 signaling (*TrkB*$^{WT/WT}$ [n=8] or *TrkB*$^{PLC/PLC}$ [n=9]) inhibits SE induced by infusion of KA into amygdala as revealed by duration of EEG seizures (A) and convulsive motor seizures (B). (D-F) Genetically disrupting PLCγ1 signaling (*PLC*$^{+/+}$ [n=8] or *PLCγ1*$^{+/-}$ [n=8]) inhibits SE induced by infusion of KA into amygdala as revealed by duration of EEG seizures (D) and

convulsive motor seizures (E). (C) and (F) are heat maps of maximum score of behavioral seizure of each mouse during 5 min observation periods following infusion of KA. The average behavioral seizure scores reported in Figures 2E and 2G represent the average of each 5 minute epoch for a given animal as presented in Figure S2C and S2F respectively. Data are presented from individual animals as well as mean and analyzed using Student's t-test, n=8-9, **p<0.01 and ***p<0.001.

**Figure S2**

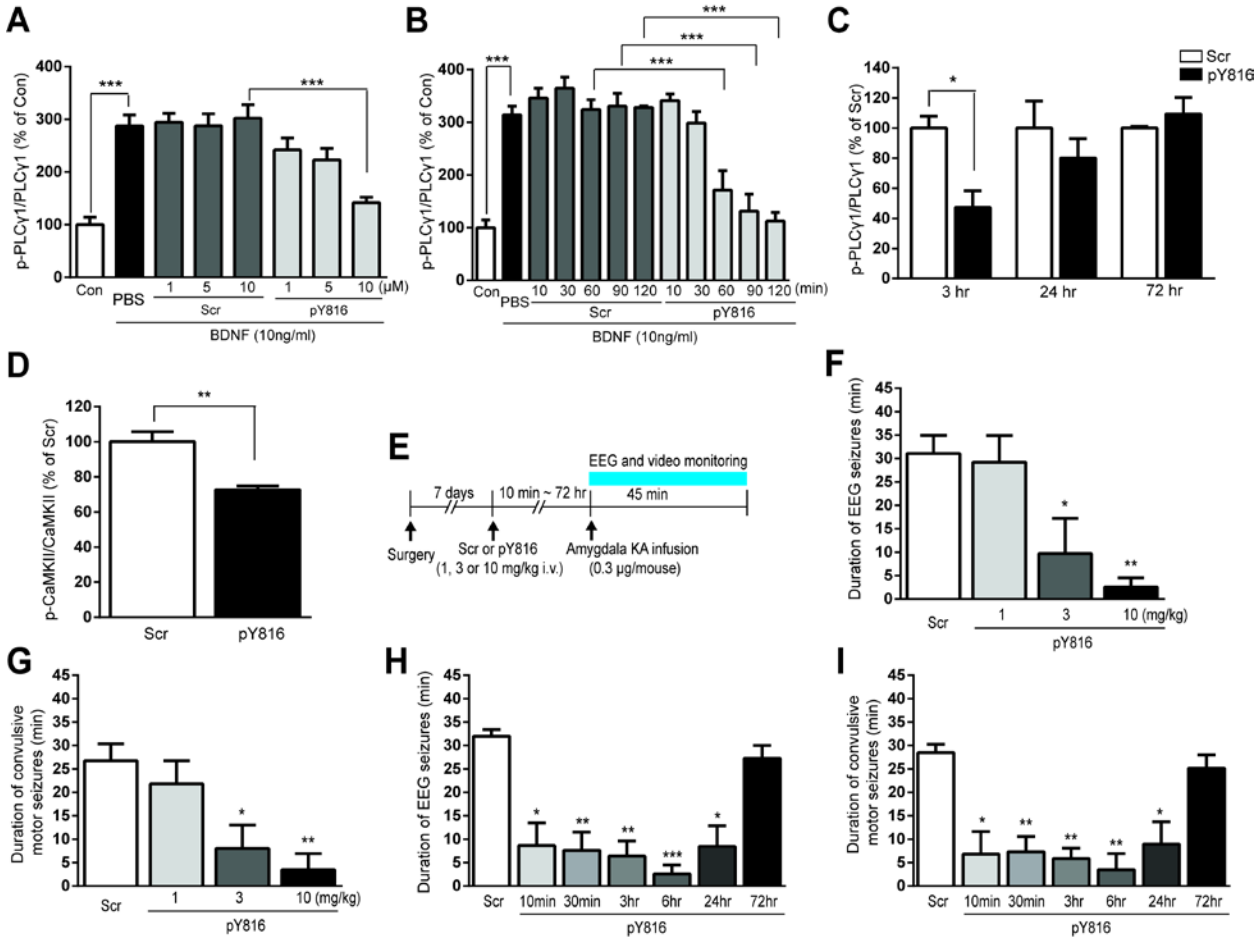


**Figure S2, Related to Figure 3. pY816 inhibits PLCγ1 activation and chemoconvulsant-induced SE.**

Either PBS or various concentrations of Scr or pY816 peptide (A) were preincubated for various periods of time (B) with cultured neurons prior to addition of BDNF (10 ng/ml). (A) and (B) present quantification of ratios of immunoreactivity of p-PLCγ1 (pY783) to PLCγ1 (n=3). Representative western blots of p-PLCγ1 (pY783) and PLCγ1 are shown in Figures 3A and 3B. (C) Scr or pY816 (10 mg/kg, i.v.) was injected into naïve mice and animals were euthanized 3, 24 and 72 hr later and hippocampal homogenates

subjected to SDS-PAGE and western blotting. In comparison to Scr control, ratios of immunoreactivity of p-PLCγ1 (pY783) to PLCγ1 show that pY816 (10 mg/kg) significantly reduces p-PLCγ1 (pY783) at 3 hr (~50%) followed by return to control levels by 72 hr (n=3-4). (D) Ratios of immunoreactivity of p-CaMKII (pT286) to CaMKII (both α and β subunits) demonstrate that systemic injection of pY816 peptide (10 mg/kg) reduces CaMKII activation at 3 hr (n=4). Representative western blots of p-CaMKII (pT286) and CaMKII were shown in Figure 3C. The effects of varying doses of pY816 or Scr peptide (1, 3 and 10 mg/kg, n=3-4; Scr control = 10) injected i.v. 6 hr prior to infusion of KA into amygdala were assessed on duration of EEG seizures (F) and convulsive motor seizures (G). The effects of a single dose of either pY816 or Scr peptide (10 mg/kg) injected i.v. at various intervals (15 min, 30 min, 3 hr, 6 hr, 24hr and 72 hr, n=3-4; Scr control = 18) prior to infusion of KA into amygdala were assessed on duration of EEG seizures (H) and convulsive motor seizures (I). Data are presented as mean ± SEM and analyzed using Two-way ANOVA with *post hoc* Bonferroni's test (A, B, C, F, G, H and I) or Student's t-test (D); *$p<0.05$, **$p<0.01$ and ***$p<0.001$.

**Figure S3**

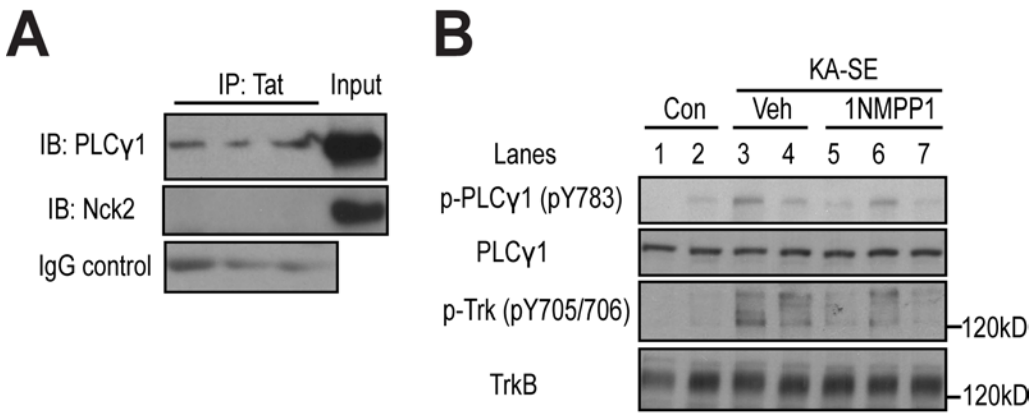


**Figure S3, Related to Figure 3. Effects of pY816 and TrkB kinase inhibition *in vivo*.**

(A) Mice were injected with pY816 peptide (10 mg/kg, i.v.) and euthanized 3 hr later. Hippocampal lysates were incubated with HIV-Tat antibody and immunoprecipitates were subjected to SDS-PAGE and western blotting. The blots were probed with antibodies to PLCγ1 or Nck2. Blot reveals co-immunoprecipitation of PLCγ1 but not Nck2, an SH2- domain containing protein that binds TrkB (Suzuki et al., 2002). (B) Western blots of p-PLCγ1 (pY783), PLCγ1, p-Trk (pY705/706) and TrkB of hippocampal lysates of *TrkB*$^{F616A}$ mice treated with vehicle or 1NMPP1 (16.6 mg/kg, i.p.) immediately following and again 1 hr after SE. Mice were euthanized 3 hr after completion of SE. Control animals underwent infusion of PBS in amygdala and were subsequently treated with vehicle. In the two vehicle treated animals undergoing KA-SE, SE resulted in activation of TrkB as evidenced by increased pY705/706 which was paralleled by enhanced activation of PLCγ1 evident in increased pY783 (compare lanes 3 and 4 with 1 and 2). In two animals in which 1NMPP1 treatment markedly inhibited SE-induced activation of TrkB (lanes 5 and 7), the SE-induced activation of PLCγ1 was also

markedly inhibited; in comparison to these two animals, the animal in which 1NMPP1 treatment only partly inhibited activation of TrkB (lane 6) exhibited greater pY783 immunoreactivity. Importantly, 1NMPP1 inhibits activation of TrkB in *TrkB*$^{F616A}$ but not wild type animals (Liu et al., 2013), demonstrating its selectivity for TrkB kinase. In sum, these correlations support the conclusion that TrkB is the dominant signaling pathway inducing PLCγ1 activation in the context of SE.

**Figure S4**

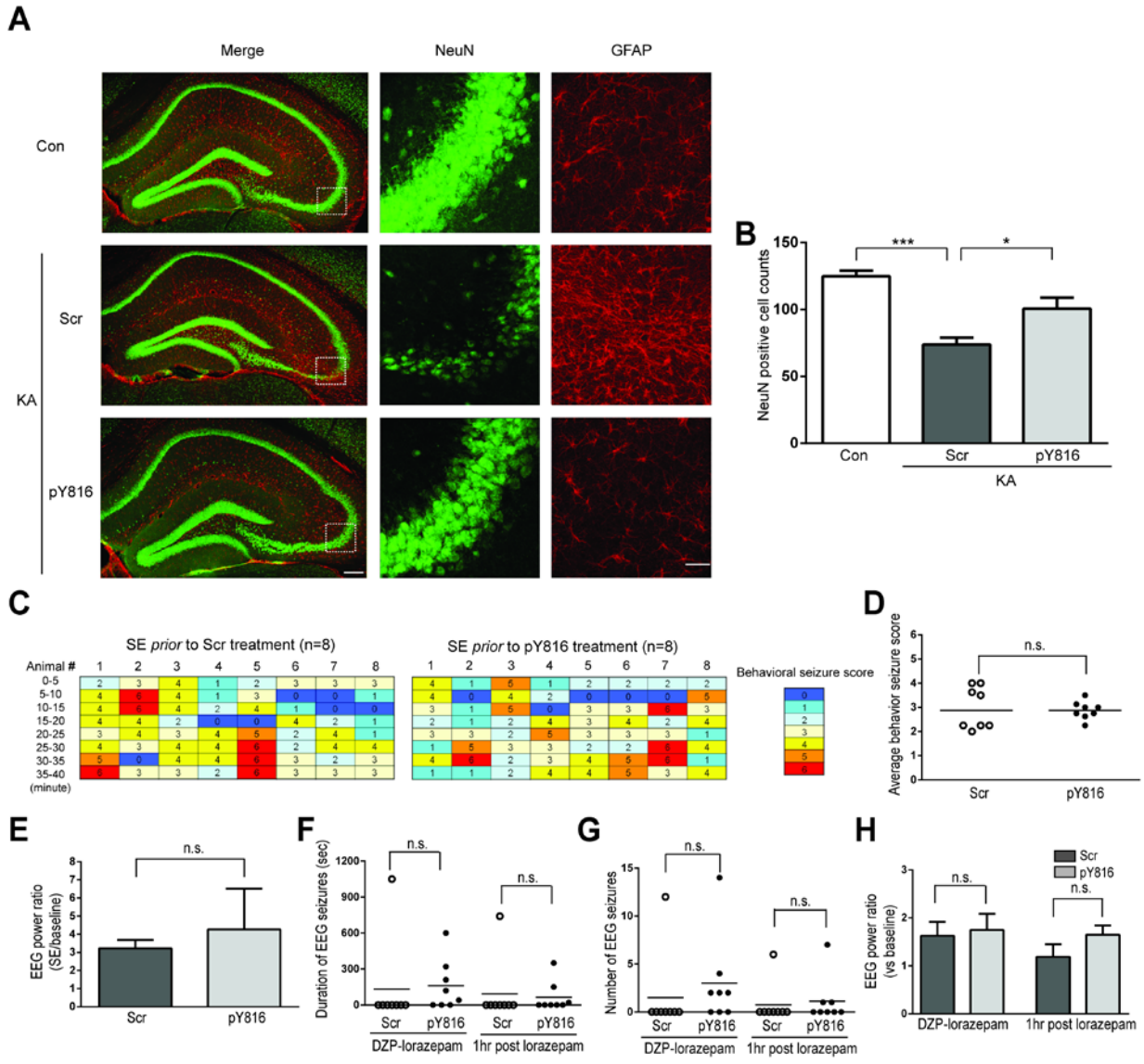


**Figure S4, Related to Figure 4. Treatment with pY816 does not modify SE induced by KA yet reduces hippocampal damage in comparison to Scr control.**

(A) and (B), Immunohistology study was performed on animals euthanized 10 weeks after KA-SE in experiment depicted in Figure 4E. (A) Representative images of immunostaining of NeuN (green) and GFAP (red) in hippocampus ipsilateral to the infusion site in control (Con, PBS infusion), KA-Scr treated, and KA-pY816 treated mice,

scale bar = 200 µm. Insets: Loss of NeuN positive cells together with reactive gliosis evidenced by enlarged GFAP-immunoreactive cells were detected in hippocampus CA3 a/b of KA-Scr treated mice (middle row). This hippocampal damage was attenuated by pY816 (bottom row), scale bar = 30 µm. (B) Number of NeuN positive cells in ipsilateral hippocampus CA3 a/b was reduced in mice undergoing KA-SE and treated with Scr thereafter compared to PBS controls ($p<0.001$). Treatment with pY816 inhibited loss of NeuN positive cells by approximately 50% in comparison to Scr control peptide (*$p<0.05$). Data are presented as mean ± SEM and analyzed using two-way ANOVA with Bonferroni *post hoc* tests, n=4-8. (C-H) Behavioral and EEG measures reveal similarity of KA-evoked SE in animals treated with Scr or pY816 following SE. These data pertain to animals in experiment depicted in Figure 4E in which a total of three doses of either Scr or pY816 were administered following SE. (C) Heat map presents the maximum behavioral seizure exhibited in 5 min intervals in each mouse prior to treatment with Scr or pY816 peptide. Average behavioral seizure scores (D) and EEG signal energy analyses (E) of SE revealed no significant differences (n.s.) between animals subsequently treated with Scr or pY816 peptide. Additional measures of duration (F) and number (G) of electrographic seizures as well as EEG power (H) revealed similar activity during 1 hr between treatment with diazepam and lorazepam and 1hr post lorazepam; note that in these experiments, either Scr or pY816 peptide was infused immediately following treatment with diazepam. Data are presented as mean ± SEM and analyzed using Student's t-test (E-H) or from individual animals as well as median and analyzed using Mann-Whitney U test (D), n=8.

## Supplemental Experimental Procedures

### Animals

*TrkB*$^{WT/WT}$ and *TrkB*$^{PLC/PLC}$ mutant mice were generated by cDNA knockin approach as described previously (Minichiello et al., 2002). In brief, PCR-based site-directed mutagenesis was used to induce a single point mutation (A to T position 2958) in TrkB cDNA that resulted in substituting phenylalanine for tyrosine 816 (Y816F), thereby disrupting the binding of PLCγ1. The mutant TrkB cDNA (*trkB*$^{PLC}$) and wild type TrkB cDNA (*trkB*$^{WT}$) were knocked into the juxtamembrane exon of the mouse *trkB* gene. *TrkB*$^{WT/WT}$ and *TrkB*$^{PLC/PLC}$ mutant mice on a C57BL/6 and 129 hybrid genetic background were back crossed to C57BL/6 for five generations. Adult male and female homozygous mutant *TrkB (TrkB*$^{PLC/PLC}$) and wild type knockin *TrkB* (*TrkB*$^{WT/WT}$) mice were used in this study.

*PLCγ1* mutant mice were generated by targeted deletion of genomic sequences encoding the X domain and both SH2 domains of *PLCγ1* as described previously (Ji et al., 1997). *PLCγ1* mutant mice on a 129/SvJ background were crossed to C57BL/6 for five generations. Note that the line generated with replacement vector TV-1 was used in these experiments (Ji et al., 1997). Homozygous disruption of *PLCγ1* (*PLCγ1*$^{-/-}$*)* results in embryonic lethality at approximately embryonic day 9.0–9.5. Therefore, adult male and female heterozygotes *of PLCγ1* (*PLCγ1*$^{+/-}$) and wild type littermates (*PLCγ1*$^{+/+}$) were used in this study. Notably, hippocampal expression of PLCγ1 protein is reduced by approximately 50% in *PLCγ1*$^{+/-}$ mice (He et al., 2014; Ji et al., 1997).

*TrkB*$^{F616A}$ knockin mutant mice were provided by Dr. David Ginty and generated as described previously (Chen et al., 2005). In brief, chimeric mice were obtained following

blastocyst injection of targeted embryonic stem cells. As a result, the *TrkB*$^{F616A}$ knockin mice harbor a single point mutation, changing phenylalanine to alanine at residue 616 within the ATP binding pocket of kinase subdomian V. This mutation renders TrkB of mutant (*TrkB*$^{F616A}$) but not wild type (WT) mice sensitive to inhibition by a blood-brain barrier permeable small molecule, 1-(1,1-dimethylethyl)-3-(1-naphthalenylmethyl)-1H-pyrazolo[3,4-d]pyrimidin-4-amine (1NMPP1). *TrkB*$^{F616A}$ knockin mice on a C57BL/6 and 129 hybrid genetic background were back crossed to C57BL/6 for one generation. Adult male and female homozygous mice (*TrkB*$^{F616A}$) were used in this study.

The genotype of each animal was assessed using polymerase chain reaction (PCR) of genomic DNA isolated from tails. Wild type C57BL/6 mice purchased from Charles River were used in some experiments. Animals were handled according to the National Institutes of Health Guide for the Care and Use of the Laboratory Animals and the experiments were conducted under an approved protocol by the Duke University Animal Care and Use Committee.

**Peptides and Reagents**

HIV-1 Tat protein transduction domain (YGRKKRRQRRR) was conjugated to the N-terminus of a sequence of human TrkB (807-820) with tyrosine residue (817 of human and 816 of mouse and rat) phosphorylated (pY816, YGRKKRRQRRR-LQNLAKASPVpYLDI). A HIV-1 Tat protein transduction domain conjugated to a scrambled peptide (Scr, YGRKKRRQRRR-LVApYQLKIAPNDLS) served as control. Peptides were synthesized and purified by Tufts Peptide Core Facility. Peptides were dissolved in phosphate-buffered saline (PBS) at a concentration of 2 mg/ml and stored at -80°C until use. Aliquots of pY816 and Scr were thawed and injected intravenously

(i.v.) shortly thereafter. All reagents were purchased from Sigma unless specified otherwise.

**Surgery and Kainic Acid (KA) Microinfusion**

Adult mice (20-25g) were anesthetized and placed in a stereotaxic frame. A guide cannula (Plastics One) was inserted above the right amygdala (coordinates from bregma: AP=-1.2 mm; L= 3.0 mm). A bipolar electrode was placed into the left dorsal hippocampus (coordinates from bregma: AP=-2.0 mm; L=-1.6 mm; and D=-1.5 mm below dura) (Figure 2A). After a 7-day postoperative recovery, animals were gently restrained and an infusion cannula (Plastics One) was inserted into the right amygdala through the guide cannula to a depth of 3.7 mm below the dura. Either KA (0.3 μg in 0.5 μl PBS) or vehicle (0.5 μl of PBS) was infused into the right amygdala at the rate of 0.11 μl/min. Following completion of the infusion, the cannula was left in the right amygdala for two additional min. Subsequently, animals were housed individually for electroencephalogram (EEG) telemetry and video monitoring.

**Status Epilepticus (SE) and Video-EEG Monitoring**

Continuous hippocampal EEG telemetry (Grass Instrument Co.) and time-locked video-monitoring were performed using Harmonie software (Stellate Systems). Monitoring started 15 min before amygdala KA infusion for recording baseline EEG and behavioral activity. Emergence of SE was typically evident in EEG recordings 0-10 min after completion of KA infusion. Behavioral seizures were classified according to a modification of Racine scale for mice (Borges et al., 2003; Racine, 1972): 0, normal activity; 1, arrest and rigid posture; 2, head nodding; 3, partial body clonus (unilateral

forelimb clonus); 4, rearing with bilateral forelimbs clonus; 5, rearing and falling (loss of postural control); 6, tonic-clonic seizures with running and/or jumping.

For experiments in which pY816 or Scr was administered prior to infusion of KA, mice were monitored for 45 min following KA infusion. EEG patterns consistent with electrographic SE included any of the following: 1. discrete electrographic seizures; 2. waxing and waning epileptiform activity; 3. continuous, high amplitude, rapid spiking; 4. periodic epileptiform discharges on a relatively flat background as described (Treiman et al., 1990; Walton and Treiman, 1988). The duration of behavioral and electrographic SE were determined by analyses of video and EEG data by trained observers blinded to treatment of mice. A similar method was used in experiments examining effects of mutations (*TrkB*$^{PLC/PLC}$ and *PLCγ1*$^{+/-}$) on SE induced by KA.

**Video-EEG Monitoring for Detection of Spontaneous Recurrent Seizures**

For experiments in which pY816 or Scr was administered following SE, diazepam (10 mg/kg, i.p.) was administered 40 minutes after the onset of SE followed by lorazepam (6 mg/kg, i.p.) one hour later to suppress SE and limit the mortality and morbidity. Animals underwent continuous video-EEG monitoring 24 hr per day, 7 days per week for the first two weeks after SE (day 1-14); at the end of the second week, monitoring was discontinued and animals were returned to home cages. After a two-week interval, monitoring was resumed for an additional two weeks (days 29-42). Spontaneous recurrent seizures were identified by review of video-EEG files independently by each of two trained readers blinded to treatment of mice. The consistency of identifying SRS between readers was ~90%; in instances in which readers disagreed, the events were excluded from this study. SRS was defined electrographically as high frequency (>5

Hz), high amplitude (>2 X baseline) rhythmic epileptiform activity with a minimal duration of 5 s. Behavioral correlates of these electrographic seizures ranged from Classes 1 through 6.

**Behavioral and EEG measures of SE both prior to and following treatment with pY816 or Scr control peptide**

Meaningful interpretation of the beneficial effects of pY816 treatment requires that the insult of SE be similar in the Scr control and pY816 groups. Analyses of the behavioral features of the SE *prior* to treatment with Scr or pY816 revealed similarity of the insult in the two groups (Figures S4C and S4D). Likewise, quantification of the EEG features as assessed by EEG power revealed similarity of the SE in the two groups (Figure S4E). In experiments assessing preventive effects of pY816, diazepam was administered to terminate SE and the first dose of pY816 was administered *after* diazepam. Although behavioral seizures were eliminated in all animals within a minute after injection of diazepam, residual seizures evident by EEG persist in some animals during the hour following diazepam and, in an occasional animal, even briefly following treatment with lorazepam one hour later (Liu et al., 2013). We therefore carefully quantified EEG seizures during the one hour interval between diazepam and lorazepam and during the one hour following lorazepam; EEG seizures were assessed by both visual inspection assessing number and duration and by computerized measurement of EEG power. No significant differences in any of these measures were detected between Scr control and pY816 peptide treated groups (Figures S4F-H). Review of continuous video-EEG recordings during the 48 hr following completion of SE by an investigator blinded to treatment revealed a single seizure in a single animal in both the pY816 and Scr control

groups (Figure 4G, top two rows). Collectively, these data reinforce the conclusion that the severity of the SE insult is similar in the two groups.

**Fluoro-Jade C (FJC) Staining**

Mice were sacrificed 24 hours after completion of SE and perfused with PBS containing heparin (1U/ml) followed by 4% paraformaldehyde. Brains were removed, frozen by slow immersion in isopentane chilled in dry ice, cryoprotected, and sectioned. Serial 40 µm coronal sections were cut through the forebrain spanning the entire hippocampus. Sections were subjected to FJC (Millipore, MA USA) staining as previously described (Mouri et al., 2008). Stained sections were examined using a ZEISS AX10 microscopy system equipped with a 10x objective lens and fluorescein filter (excitation: 485 nm; emission: 525 nm). The number of FJC positive cells were counted in two adjacent sections from middle level (AP from Bregma: −1.82 mm) of hippocampus ipsilateral to KA infusion site by an observer blinded to genotype and treatment conditions with ImageJ software (Ferreira and Rasband, 2011) in a 260 X 260 µm field within hippocampal CA1 or CA3 a/b subfield.

**Cell Culture**

Dissociated neuronal cultures were prepared as described previously (Huang et al., 2008). Briefly, cortical mixed neuron and glia cultures were prepared from pups of E18 pregnant Sprague Dawley rats (Charles River). Cells were cultured in Neurobasal with B27 supplement for 10-12 days *in vitro* (DIV) before use. Medium was replaced with artificial cerebrospinal fluid (ACSF) buffer *before* BDNF (10 ng/ml, Chemicon) stimulation. Following a 15 min incubation in presence of BDNF, cells were lysed in modified RIPA buffer (20 mM Tris, pH 7.5, 137 mM sodium chloride, 1% NP40, 0.25%

sodium deoxycholate, 1 mM sodium orthovanadate, 1 mM PMSF, and one complete Mini protease inhibitor cocktail tablet [Roche]/10 ml), briefly centrifuged, and the supernatant was used for western blotting.

**Immunoprecipitation**

Animals were anesthetized with pentobarbital (200 mg/kg i.p.) and decapitated, and the head was quickly immersed in liquid nitrogen for 4 s to rapidly cool the brain. The hippocampi were rapidly dissected on ice and homogenized in modified RIPA buffer, incubated on ice for 15 min, and centrifuged at ~200,000 x g for 10 min at 4°C. The supernatant was collected and stored at -80°C. Hippocampal lysates (1 mg) were incubated with TrkB (1 µg, Millipore) and HIV-Tat (2 µg, Thermo Scientific) antiboddies respectively. The lysates were incubated with 100 µL of protein A-Sepharose beads (Roche) overnight at 4°C. The beads/immune complexes were pelleted in a microcentrifuge and then resuspended in RIPA buffer and this procedure was repeated two additional times before adding 2 x SDS PAGE sample buffer and boiled. The western blots were prepared and probed with TrkB (1:1000, Millipore) or PLCγ1 (1:500, Cell signaling) for TrkB immunoprecipitation and PLCγ1 or Nck2 (1:500, BD Transduction Laboratories) for HIV-Tat immunoprecipitation respectively.

**Western Blotting**

Western blotting was conducted as previously described (He et al., 2010). Cell lysates and hippocampal homogenates were subjected to SDS-PAGE, transferred, and blots probed with antibodies (1:1000, Cell signaling unless otherwise noted) to the following: p-PLCγ1 (pY783), PLCγ1, p-CaMKII (pT286) (Abcam), CaMKII, p-Akt (pS473), Akt, p-S6 ribosomal protein (pS235/236), S6 ribosomal protein, p-ERK1/2 (Thr202/Tyr204),

ERK, p-Trk (705/706) (Santa Cruz) and TrkB (Millipore). The immunoreactivity of individual bands on western blots was measured by ImageJ software (National Institutes of Health) and normalized to immunoreactivity of PLCγ1, CaMKII (both α and β subunits), Akt, S6 or ERK respectively. Equivalent protein loading and transfer were monitored by β-actin (1:10000, Sigma) immunoreactivity. Shown are representative results of immunoblotting from at least three independent experiments.

**Behavior Tests**

*Open Field Test.* A plexiglas arena (40 x 40 x 40 cm) was placed in a room with homogenous illumination (~ 300 lux). The arena was subdivided into sixteen 10 x 10 cm squares by lines marked on the floor. Each mouse was placed in the center of the open field and allowed to freely explore the apparatus for 5 minutes. A video camera mounted directly above the arena was used to monitor animal activity and movement. To assess locomotor activity, an investigator unaware of the treatment reviewed the video and recorded line crossing (frequency of crossing grid lines with all four paws) and the frequency of rearing (standing on hind legs or leaning against the walls of the arena).

*Light/Dark Box Test*. The apparatus (20 x 40 x 40 cm) consisted of two acrylic compartments. The dark compartment (30 x 40 cm) and light compartment (40 x 40 x 40 cm, brightly illuminated at 600 lux) were separated by a divider with a 5.5 x 5.5 cm opening at floor level. Mice were placed into the dark side and allowed to move freely between the two chambers with the door open for 5 minutes. During behavior tests, a video camera mounted directly above the arena was used to monitor animal activity and a blinded investigator determined the latency to first entry into lighted compartment

(entering the lighted side with all four paws) and the total time spent on the lighted side to assess anxiety-like behavior in light/dark box test.

**Quantitative Analysis of EEG Energy Content**

Quantitative analysis of EEG energy content was performed using the method described previously (Lehmkuhle et al., 2009; Liu et al., 2013). Experimental design necessitated handling the animals (e.g. KA microinfusion, treatment with benzodiazepine or peptide) which resulted in EEG artifacts. EEG records were reviewed to detect these artifacts and these portions of recording were removed. To assure objectivity, detection and removal of such artifacts from power plots and corresponding EEG and subsequent analyses were performed by an investigator unaware of either treatment or genotype. We calculated running power in the gamma band (20-50 Hz) at a one-second resolution and smoothed the resulting time-series using a 5 min moving average filter. We averaged the values of the smoothed gamma power time-series during and following the period of SE and normalized it to the average of the baseline to give ratios representing gross activity.

**Immunohistochemistry**

Mice were deeply anesthetized and perfused with PBS containing heparin (5U/ml) followed by buffered 4% paraformaldehyde. Brains were removed, frozen by slow immersion in isopentane chilled in dry ice, cryoprotected, and sectioned. Serial 40 µm coronal sections were cut through the forebrain spanning the entire hippocampus. Adjacent sections at middle level of hippocampus (AP from Bregma: −1.82 mm) were subjected to immunofluorescent staining. Neurons and astrocytes were visualized using antibodies against neuronal nuclei (mouse monoclonal to NeuN, 1:500; Millipore) and

glial fibrillary acidic protein (rabbit polyclonal to GFAP, 1:500; Sigma) detected with Alexafluor 488 coupled anti-mouse and Alexafluor 594 coupled anti-rabbit secondary antibodies (Molecular Probes), respectively. Images were captured using a Leica TCS SL confocal microscopy system equipped with a 63x oil-immersion objective lens. NeuN-positive cell counting was performed by an investigator blinded to the treatment conditions with ImageJ software (Ferreira and Rasband, 2011) in a 260 X 260 µm field within the CA3b pyramidal cell layer. Mean counts were obtained from two adjacent sections ipsilateral to the infused site.

**Statistical Analysis**

Statistical analysis was performed with Prism 5 software (GraphPad Software Inc.). Sample sizes were chosen based on power analysis. Detailed information regarding sampling and normalization is described in the figure legends. Unless otherwise noted, all values in figures are presented as means ± SEM. Unless otherwise noted, comparisons between two groups were analyzed using unpaired Student's t-tests, while multi-group comparisons were analyzed using two-way ANOVA followed by Bonferroni *post-hoc* tests. A $p < 0.05$ was considered significant.

**Supplemental References**

Borges, K., Gearing, M., McDermott, D.L., Smith, A.B., Almonte, A.G., Wainer, B.H., and Dingledine, R. (2003). Neuronal and glial pathological changes during epileptogenesis in the mouse pilocarpine model. Exp Neurol *182*, 21-34.

Chen, X., Ye, H., Kuruvilla, R., Ramanan, N., Scangos, K.W., Zhang, C., Johnson, N.M., England, P.M., Shokat, K.M., and Ginty, D.D. (2005). A chemical-genetic approach to studying neurotrophin signaling. Neuron *46*, 13-21.

Ferreira, T., and Rasband, W. (2011). The mageJ User Guide.

He, X.P., Pan, E., Sciarretta, C., Minichiello, L., and McNamara, J.O. (2010). Disruption of TrkB-mediated phospholipase Cgamma signaling inhibits limbic epileptogenesis. J Neurosci *30*, 6188-6196.

He, X.P., Wen, R., and McNamara, J.O. (2014). Impairment of kindling development in phospholipase Cgamma1 heterozygous mice. Epilepsia *55*, 456-463.

Huang, Y.Z., Pan, E., Xiong, Z.Q., and McNamara, J.O. (2008). Zinc-mediated transactivation of TrkB potentiates the hippocampal mossy fiber-CA3 pyramid synapse. Neuron *57*, 546-558.

Ji, Q.S., Winnier, G.E., Niswender, K.D., Horstman, D., Wisdom, R., Magnuson, M.A., and Carpenter, G. (1997). Essential role of the tyrosine kinase substrate phospholipase C-gamma1 in mammalian growth and development. Proceedings of the National Academy of Sciences of the United States of America *94*, 2999-3003.

Lehmkuhle, M.J., Thomson, K.E., Scheerlinck, P., Pouliot, W., Greger, B., and Dudek, F.E. (2009). A simple quantitative method for analyzing electrographic status epilepticus in rats. J Neurophysiol *101*, 1660-1670.

Liu, G., Gu, B., He, X.P., Joshi, R.B., Wackerle, H.D., Rodriguiz, R.M., Wetsel, W.C., and McNamara, J.O. (2013). Transient Inhibition of TrkB Kinase after Status Epilepticus Prevents Development of Temporal Lobe Epilepsy. Neuron *79*, 31-38.

Minichiello, L., Calella, A.M., Medina, D.L., Bonhoeffer, T., Klein, R., and Korte, M. (2002). Mechanism of TrkB-mediated hippocampal long-term potentiation. Neuron *36*, 121-137.

Mouri, G., Jimenez-Mateos, E., Engel, T., Dunleavy, M., Hatazaki, S., Paucard, A., Matsushima, S., Taki, W., and Henshall, D.C. (2008). Unilateral hippocampal CA3-predominant damage and short latency epileptogenesis after intra-amygdala microinjection of kainic acid in mice. Brain Res *1213*, 140-151.

Racine, R.J. (1972). Modification of seizure activity by electrical stimulation. II. Motor seizure. Electroencephalogr Clin Neurophysiol *32*, 281-294.

Suzuki, S., Mizutani, M., Suzuki, K., Yamada, M., Kojima, M., Hatanaka, H., and Koizumi, S. (2002). Brain-derived neurotrophic factor promotes interaction of the Nck2 adaptor protein with the TrkB tyrosine kinase receptor. Biochemical and biophysical research communications *294*, 1087-1092.

Treiman, D.M., Walton, N.Y., and Kendrick, C. (1990). A progressive sequence of electroencephalographic changes during generalized convulsive status epilepticus. Epilepsy research *5*, 49-60.

Walton, N.Y., and Treiman, D.M. (1988). Response of status epilepticus induced by lithium and pilocarpine to treatment with diazepam. Exp Neurol *101*, 267-275.